Early-age reactivity and strength development in high volume mine tailings-based alkali activated binders and their application potential

Rijul Kanth Ramasamy Jeyaprakash¹, Sahil Surehali^{1*}, Aswathy Simon¹, Taihao Han², Aditya Kumar³, Narayanan Neithalath⁴

Abstract:

Mine tailings (MT) present environmental and health risks, necessitating suitable waste management strategies to safely dispose them. One of the most effective methods to immobilize detrimental ingredients present in tailings, yet at the same time synthesize value-added materials in large volumes, is through the development of cementitious binders containing tailings. In this work, copper mine tailings are used to develop alkali-activated binders for several construction-related applications. The binders are designed with \geq 70% by mass of MT, along with minor additions of reactive materials such as cement (C) or slag (S), to obtain 28-day compressive strengths of up to 40 MPa when cured under ambient conditions, contrary to low strength MT-based binders that are generally reported. Setting time is used as a simple criterion to screen the mixtures. The influence of varying Na₂O-to source material (MT + cement/slag) ratio (n) and SiO₂-to-Na₂O ratio (n) of the activator on the calorimetric response, flow, and compressive strength development are studied in detail. MT-S blends demonstrate higher strengths (up to 40 MPa) as compared to MT-C blends (up to 12 MPa). Lower n_s and higher n values lead to higher strengths for MT-S blends, while a higher n_s yields better strength for MT-C blends. Based on the binder strength, application avenues such as structural/non-structural masonry, pre-cast non-structural/structural panels, and grouts are identified.

Keywords: Alkali activation; mine tailings; slag; cement; calorimetry; strength development

Corresponding author: e-mail: $\underline{ssurehal@asu.edu}$

 $^{^{\}rm I}$ Graduate student, School of Sustainable Engineering and Built Environment, Arizona State University, Tempe AZ 85287

² Postdoctoral researcher, Department of Materials Science and Engineering, Missouri University of Science and Technology, Rolla, MO 65409

³ Associate Professor, Department of Materials Science and Engineering, Missouri University of Science and Technology, Rolla, MO 65409

⁴ Professor, School of Sustainable Engineering and Built Environment, Arizona State University, Tempe AZ 85287;

1. Introduction

Mine tailings (MT) are residue materials discharged after separating valuable ores in mining operations. A significant amount of mine tailings are produced globally (~5-7 billion tons (R.S. Krishna et al., 2021; Qaidi et al., 2022)), making their sustainable disposal a critical environmental challenge. The physical and chemical properties of tailings are dependent on the type of ore extracted, their location and exposure conditions, and the methods used for extraction and processing. For instance, porphyry copper deposits that have been exposed to weathering for a long time may also contain secondary copperbearing minerals like azurite (Cu₃(CO₃)₂(OH)₂), atacamite (Cu₂Cl(OH)₃), cuprite (Cu₂O), etc., in addition to the primary copper-bearing sulfide minerals, such as chalcopyrite (CuFeS₂), chalcocite (Cu₂S), bornite (Cu₃FeS₄), and enargite (Cu₃AsS₄) (Tabelin et al., 2021b). Considerable variations in the properties of tailings extracted from different ore types are reported in the literature (Calderon et al., 2020; Marove et al., 2022; Opiso et al., 2023; Tabelin et al., 2021a, 2020).

MT wastes, which are usually disposed of in surface reservoirs or tailings storage facilities (Tabelin et al., 2022), are known to result in serious environmental impacts including the rendering large land areas waste, generation of windblown dust, chemical contamination of surface- and ground-water, and potential for loss of life and ecological damage in the event of collapse of tailings storage facility (Akinyemi et al., 2022; Jamshidi-Zanjani and Saeedi, 2013; Provis, 2018). The disposal of mine tailings also contributes to soil pollution and detrimentally influences the flora due to the leaching of heavy metals, process reagents, and sulfur compounds (Hageman and Briggs, 2000; L. Jiang et al., 2021; X. Jiang et al., 2021; Zhang et al., 2020). Mine tailings that contain sulfide minerals, by virtue of its oxidation, will form sulfuric acid, which when remain uncaptured, leads to acid mine drainage (Ruiz-Sánchez et al., 2023). Copper mining and processing (from which the tailings used in this study are obtained) can expose or concentrate naturally occurring radioactive materials (NORM; e.g., radium, uranium, thorium, and their radioactive decay products), transforming them into technologically enhanced NORM (TENORM) (US EPA, 2014). Moreover, production of 1 t of copper requires ~150 t of ore to be excavated, crushed, and chemically treated, thereby producing large amounts of tailings that could contain toxic metals and metalloids (Rzymski et al., 2017). The disposal of MT thus is an environmental liability, resulting in mining operators and environmental agencies investing in sustainable tailings-waste management methods that focus on valorizing these waste materials through their reuse and recycling.

Some of the commonly adopted methods that potentially reduce the environmental impacts associated with MT are: a) chemical stabilization by the addition of certain chemicals or encapsulating them in cementitious materials to immobilize the heavy metals; b) better ore extraction methods by preconcentration methods, by-product recovery, and avoiding "high grading", which refers to choosing a high cut-off grade ore, resulting in a significant part of the mineral resource being left behind and potentially sterilized; and c) inhibiting mineral-water interactions by using phospholipids to form hydrophobic coatings on sulfide minerals to prevent acid mine drainage (Akinyemi et al., 2022; Lèbre et al., 2017; Liu et al., 2022; Niu et al., 2022; Park et al., 2019). An emerging trend in sustainable disposal of MT is their recycling in applications such as construction materials, fertilizers, glasses and ceramics, and automobile catalytic convertors (Araujo et al., 2022; Guo et al., 2018). Recent studies have explored the possibility of incorporating MT in binders such as inorganic polymers as well as those based on ordinary Portland cement (OPC) (Alonso et al., 2018; Ercikdi et al., 2017; Rao and Liu, 2015). These simple yet effective methods are expected to help develop systematic waste management practices for MT that mitigate their adverse environmental impacts.

The use of MT as an ingredient in mass-produced construction materials has gained significant attention recently (Barzegar Ghazi et al., 2022; Saedi et al., 2022; Surehali et al., 2024, 2023; Zhu et al., 2022). When used to partially replace OPC (which has significant CO₂-and-energy implications), the end product is generally a more sustainable material. However, their low reactivity (Obenaus-Emler et al., 2020) is a detriment in using them as a binder constituent, even though they can be used as filler

materials. Alkali activation, therefore, has been implemented as a potential strategy to enhance the reactivity of mine tailings, similar to that of common aluminosilicate precursors (e.g., slag or fly ash) (Bakharev et al., 2003; Bernal et al., 2012; Fernández-Jiménez et al., 1999; Kovalchuk et al., 2007; Pacheco-Torgal et al., 2012). Since most MT comprise alumina and silica that are essential for alkaline activation (Akinyemi et al., 2022; Kiventerä et al., 2020; R. S. Krishna et al., 2021; Liu et al., 2022; Xiaolong et al., 2021), it is plausible that this strategy could lead to the production of sustainable construction materials. Additionally, presence of calcium in some MT contributes to the formation of hydration products such as calcium silicate hydrate and calcium aluminate silicate hydrate (Aseniero et al., 2018; Opiso et al., 2021). Furthermore, stable reaction products such as alkali (or alkaline earth) aluminosilicates are more likely to permanently immobilize harmful ingredients and prevent them from leaching out into the environment (Tian et al., 2020; Van Jaarsveld et al., 1997; Zhang et al., 2022).

This study, therefore, develops MT-based binding materials comprising more reactive materials such as OPC or slag as minor constituents, to achieve desirable fresh and hardened properties. This work focuses on the use of MT for applications such as non-structural (e.g., insulating) and structural masonry, pre-cast non-structural and structural panels, and grouts. The novelty of this work is that it identifies optimal binder compositions and activation parameters for the appropriate application, rather than focusing on binders with a prescribed strength. Sodium silicate (waterglass) is used as the primary activating agent, along with NaOH to provide desired levels of alkalinity. Several studies that deal with activation of MT report 28-day compressive strengths of ≤5 MPa (even after mechano-thermal activation and/or the use of highly aggressive activating agents) (Koohestani et al., 2021; Ouffa et al., 2022; Perumal et al., 2020), which is inadequate for many normal- to high-performance applications mentioned above, thereby necessitating the use of a highly reactive constituent in minor quantities. The MT-slag blends developed in this study (containing ≥70% by mass of MT) demonstrate desirable setting times and flowability, and attain 28-day strengths of up to 40 MPa when cured under ambient conditions, facilitating their use in a wide variety of value-added applications in the construction domain. Since slag, a processed waste material from iron and steel production, has a lower environmental impact than OPC, and given that MT that otherwise causes harmful impacts is activated and encapsulated, the approach described here has the potential to be a highly sustainable approach for MT utilization. In addition to significantly reducing the cement content in binders for such applications, this approach also attempts to establish MT as an alternate material to resources such as fly ashes (which is the most common source material for geopolymeric binders) which are becoming scarce due to the closure of coal-fired thermal power plants in many parts of the U.S. Furthermore, the screening and test methods, and classification schema adopted in this study can likely be used in the beneficial use of other types of tailings as well.

2. Experimental program

2.1. Materials

The primary binding material used in this study was mine tailings from a copper mine, provided by Freeport McMoRan Inc. (FMI). The extraction of copper from its ore produces two types of wastes – copper slag and copper tailings. The tailings were obtained in a slurry form. They were dewatered, oven dried at 80°C for 24 h, and crushed into a fine powder before using it in the paste and mortar mixtures. Ground granulated blast furnace slag (GGBFS) conforming to ASTM C 989, and Type I/II ordinary Portland cement (OPC) conforming to ASTM C 150 were used to replace 10%, 20%, and 30% by mass of MT in the binder system, ensuring that the tailings remained the major component of the binders. The specific gravities of the binder constituents were determined using a gas pycnometer in accordance with ASTM D 5550, while a Blaine's air permeability apparatus conforming to ASTM C 204 was used to measure the powders' fineness. The chemical composition and physical properties of the binder constituents used in this study are summarized in Table 1, as obtained using X-ray fluorescence (XRF). The copper MT does not contain any detectable Ca, but has a combined (SiO₂ + Al₂O₃ + Fe₂O₃) > 85%,

meeting the chemical requirements of fly ash as per ASTM C 618. X-ray diffraction (XRD) patterns of the starting materials are shown in Figure 1. For GGBFS, an asymmetric diffuse band of glass is observed between 2θ of 20° and 37° , with the peak at 31° . The XRD patterns show that GGBFS is more amorphous, which reportedly indicates better reactivity as compared to materials like fly ash, which contains silica and alumina crystalline phases (Ravikumar et al., 2010). MT shows the presence of albite, gypsum, and quartz, which is in line with the results reported in previous studies (Ahmari et al., 2012; Ahmari and Zhang, 2012; Yu et al., 2017). Figure 2 shows the particle size distribution of the binder ingredients, determined using a laser particle size analyzer. The median particle sizes (d_{50}) were $38.63 \mu m$, $12.33 \mu m$, and $15.23 \mu m$ for mine tailings, slag, and OPC respectively. Sodium silicate solution (waterglass), with SiO₂-to-Na₂O mass ratio (referred to as M_s) of 1.59 was used as the activating agent. NaOH solution was added to the activator to reduce its M_s values to 1.0 and 1.5 (to enable efficient activation), in line with previously reported work on alkali activated binders (Dakhane et al., 2016; Vance et al., 2014).

Table 1: Chemical composition and physical properties of the binder ingredients.

Binder ingredients		Chemical composition									Physical properties	
Mine tailings <mark>#</mark>	SiO ₂ (%)	Al ₂ O ₃ (%)	SO ₃ (%)	Fe ₂ O ₃ (%)	Sn (%)	Mn (%)	Ti (%)	Sb (%)	P (%)	Sp. gravity	Blaine's Fineness (cm ² /g)	
	64.2	19.95	1.94	8.26	1.35	0.81	0.48	2.49	0.15	2.76	898	
					MgO (%)	Na ₂ O (%)	K ₂ O (%)	CaO (%)	LOI* (%)			
GGBFS	39.4	8.49	2.83	0.37	12.05	0.27	0.80	35.53	1.31	2.92	3950	
OPC	21.3	3.78	2.88	3.75	1.77	0.25	0.17	63.83	1.34	3.20	4000	

^{*}Loss on Ignition

^{# -} Heavy elements such as As, Ba, Cd, Cr, Pb, Se, and Ag were also detected in trace quantities in the mine tailings.



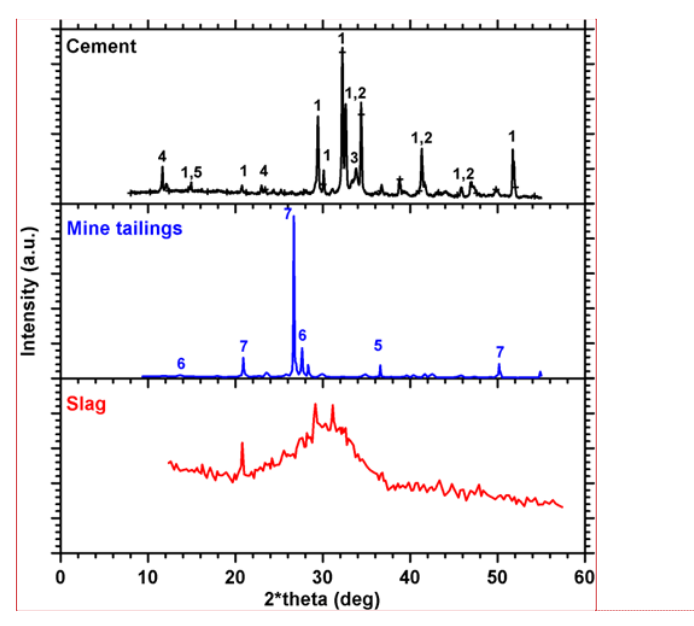


Figure 1: X-ray diffractions patterns of mine tailings, slag, and cement (1: C₃S, 2: C₂S, 3: C₃A, 4: C₄AF, 5: gypsum, 6: albite, 7: quartz).

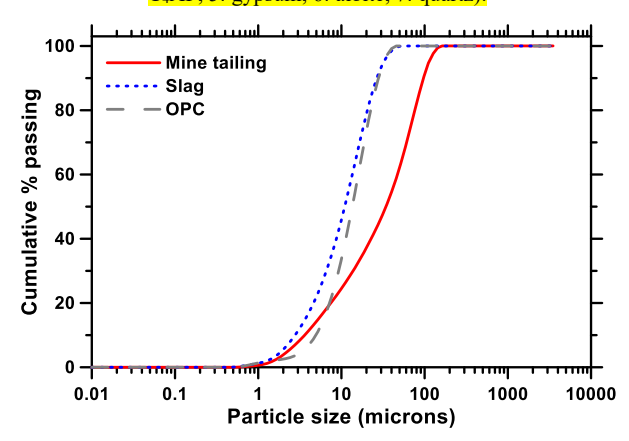


Figure 2: Particle size distribution curves for mine tailings, slag, and cement.

2.2. Mixture proportions

As mentioned earlier, slag (S) and cement (C) were used to replace 10%, 20%, and 30% by mass of MT, to develop MT-S and MT-C blends, respectively in this study. The liquid activator solution, comprising sodium silicate, NaOH, and water, was proportioned to have Na₂O-to-total powder ratio (n values) ranging from 0.025 to 0.10 in increments of 0.025, and SiO₂-to-Na₂O ratios (M_s) of 1.0 and 1.5. An l/b ratio of 0.35 was used for all the MT-S blends. For MT-C blends, l/b ratios of 0.40, 0.45, and 0.55 were used for blends with 10%, 20%, and 30% cement content by mass, respectively, to ensure that the pastes do not set during the mixing phase, and no excessive bleeding takes place after mixing.

Initially, the NaOH solution was prepared and allowed to cool down to ambient temperature to ensure that the heat released due to the exothermic dissolution of NaOH in water does not interfere with the calorimetry test results. As-obtained sodium silicate solution (provided by PQ Corp) with an M_s value of 1.59 was added to the NaOH solution to arrive at desired M_s values of 1.0 and 1.5. The activator solution was then mixed with the binder ingredients. A sample calculation of the quantities of the materials for an n value of 0.025 and an M_s value of 1.0 is detailed here. For 1000 g of powder, 25 g of Na₂O is needed to get an n value of 0.025, and 25 g of SiO₂ to obtain an M_s of 1.0. In order to obtain 25 g of SiO₂, 40.72 g of sodium silicate with an M_s of 1.59 (the liquid in sodium silicate solution needs to be accounted for) is needed. A further 9.28 g of Na₂O is needed to obtain an n value of 0.025, which is provided by 11.97 g of NaOH. Water from NaOH is 2.69 g, and that from sodium silicate solution is 54.96 g; hence the remaining water required for a l/b ratio of 0.35 is 292.4 g, which needs to be added externally. The mortar mixtures prepared for compressive strength tests comprised 50% by volume of river sand.

2.3. Test methods

The setting times of the pastes were determined using the Vicat needle method in accordance with ASTM C 191. A mini-slump cone with a height of 57 mm, and top and bottom diameters of 19 mm and 38 mm respectively, was used to quantify the flowability of the mixtures. Images of slump flow were taken from a constant height 30 s after smoothly lifting the mini-slump cone, and the spread diameters were determined from the images using Image J software. The final spread diameter reported for each mix is the average of at least four measurements.

Isothermal calorimetry experiments were carried out in accordance with ASTM C 1679. The pastes were mixed externally and loaded into the isothermal calorimeter. The time elapsed between the instant the activating solution was added to the powder and the paste loaded into the calorimeter was around 1 min. The tests were run for 48 h with the calorimeter set at a constant temperature of 25°C. The compressive strengths of the selected binders were determined in accordance with ASTM C 109. 50 mm cubes were moist-cured in a chamber at 23±2 °C and >98% RH, and tested at four different ages (3, 7, 14, and 28 days). At least three specimens from each mixture were tested for strength. Since the focus of this paper is on the early- and later-age mechanical properties of MT-based binders, other tests of significance when using materials such as MT are not discussed here. For instance, leaching of heavy metals from MT-based binders, and the influence of pore structure and microstructure on durability characteristics are not reported here and are subjects of forthcoming work.

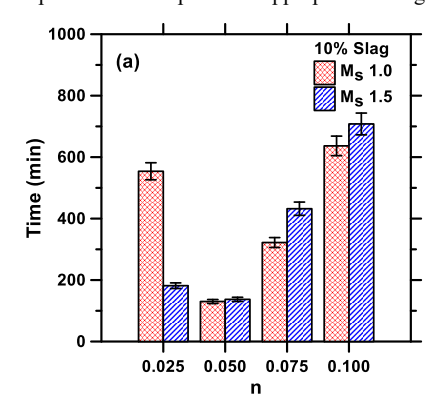
3. Results and discussion

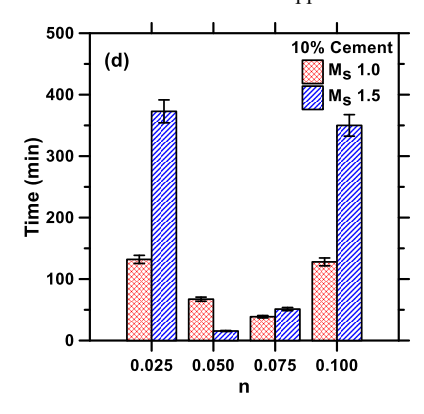
3.1. Setting times

The purpose of this work is to develop alkali activated binders that contain tailings as the primary constituent (and slag or cement as minor constituents to enhance reaction kinetics and adequate product development), such that the activated blends can attain acceptable mechanical properties under ambient moist curing conditions. Initial setting time was used as a screening criterion to select acceptable binder compositions, and activation parameters to be used for compressive strength tests. Binders with an initial setting time of less than 30 min were not selected due to their fast-stiffening nature. Additionally, binders that had final setting time greater than 12 h were also not selected for further tests.

The initial setting times for all MT-S and MT-C blends explored in this study are shown in Figure 3. The setting times decrease with an increase in the content of slag or cement, since slag and cement provide Ca²⁺ ions that combine with [SiO₄]⁴⁻ ions liberated from sodium silicate, enhancing the amount of early reaction product formation (Jiang et al., 2022; Shi and Day, 1995). The Na₂O-to-total powder ratio (*n* value) has a significant effect on the setting times, as has been described in our previous work on pure fly ash or slag-based activated binders (Dakhane et al., 2017; Ravikumar and Neithalath, 2012).

It can be seen from Figure 3 that the MT-S and MT-C blends demonstrate faster initial setting for certain n values for a particular slag and cement content and M_s value. Lower or higher n values than the optimum increases the setting time. It is well understood that when a highly alkaline solution comes into contact with the binder constituents (here, comprising MT and slag/cement), it helps to break the bonds and liberate ionic species, which on reaction, facilitate early setting (Koohestani et al., 2021; Lakrat et al., 2022; Song and Jennings, 1999). The initial setting time is delayed as the system alkalinity increases beyond a certain n value, indicating that there is a specific pH range that enables faster setting (Koohestani et al., 2021). This is because: (i) a higher than optimal pH increases the concentration of Si and Al in solution, but reduces that of Ca, and (ii) the increased amount of silicates in the activator solution retards the precipitation kinetics of the aluminate phases in slag and cement (Jiang et al., 2022; Koohestani et al., 2021) (note that for any n value, more sodium silicate is needed to provide the desired Na₂O content, and the amount over and above that is provided by NaOH). Figures 3 (a), (b), and (c) show that at M_s values of 1.0 and 1.5, the initial setting times of MT-S blends are lowest at an n value of 0.05. For MT-C blends, the initial setting time is the lowest for blends with 10% cement content at nvalues of 0.075 and 0.05 for M_s of 1.0 and 1.5 respectively. At higher cement contents of 20% and 30%, a higher n value of 0.075 results in the mixtures setting early. A proper understanding of the dependence of initial setting time on binder constituents and activator parameters allows for the tuning of the mixture proportions of alkali activated mine tailing blends for desired applications. The final setting times (not shown here for brevity) also indicate a similar trend with respect to the influence of n and M_s values. In general, the MT-S blends demonstrate a higher final setting time, allowing it to be transported and placed, when used as grouting materials, flowable fills, or for patching applications. For MT-C blends, the setting occurs much faster, especially at 20% and 30% cement contents, allowing them to be used as rapid-setting grouts and repair mortars. An in-depth evaluation of the setting process of these systems helps in the development of appropriate tailings-dominant binders for desired end-applications.





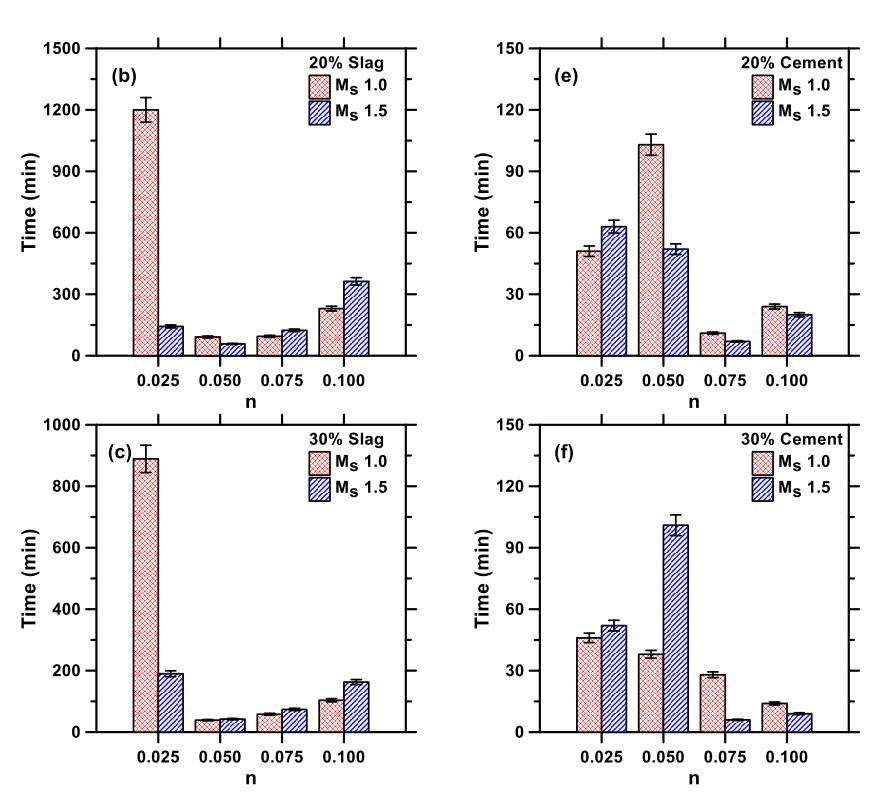


Figure 3: Initial setting times for MT-S blends with slag contents of: (a) 10%, (b) 20%, (c) 30%; and for MT-C blends with cement contents of: (d) 10%, (e) 20%, (f) 30%.

3.2. Fluidity of the mixtures

Table 2 presents the spread diameters obtained from the mini-slump tests on MT-S and MT-C blends. For the MT-S blends, fluidity is found to be rather invariant of the n and M_s values, especially for n values ≥ 0.05 , even though the l/b ratios were the same for all the slag-containing blends. For the MT-C blends, the flow values are comparable to those of the MT-S blends, for n values of 0.075 and 0.10. One of the plausible reasons for this behavior is the rheological response of the activator solutions. It has been reported that both ionic and colloidal silica species are present in these solutions (Lee and Stebbins, 2003). Decreasing the M_s of the solution (to values of 1.0 and 1.5 used in this work) requires the increased addition of NaOH. NaOH breaks the Si-O-Si chains in the polymerized colloidal silicate species in the solution, resulting in decreased molecular size and a decrease in determined activator viscosity, due to decreased colloidal particle size. This makes both the MT-S and MT-C blends more fluid at higher n values. At higher n values, there is little influence of the cement or slag content of mixtures (except for 30% cement content, where the higher alkalinity and increased cement content results in rapid hardening) on their flowability, and hence mixture proportions could be selected purely based on reactivity and strengths, considering the l/b ratios chosen in this work. The mixtures with higher fluidity can be used for self-levelling and flowable grout applications.

Table 2: Mini slump diameters (mm) of binders with slag contents of 10%, 20%, 30%, and for binders with cement contents of 10%, 20%, and 30%.

		Mass percentage of slag / cement in respective blends								
Binder system		10	%	20%		30%				
	Activation parameters	M_s								
2,2222	(n, M_s)	1.0	1.5	1.0	1.5	1.0	1.5			
	n	Mini slump diameter (mm)								
Mine tailings (MT) – slag (S)	0.025	91	96	87	74	80	56			
	0.050	106	103	114	107	115	113			
	0.075	104	102	106	106	103	110			
	0.100	100	104	104	104	104	99			
Mine tailings (MT) - cement (C)	0.025	92	79	102	109	121	131			
	0.050	53	95	93	-	128	119			
	0.075	119	114	115	124	45	-			
	0.100	115	113	123	121	96	158			

Note: (-) represents mixtures that had zero slump

3.3. Isothermal calorimetry

The heat flow and cumulative heat release curves for MT-S and MT-C blends containing 70% MT by mass are shown in Figures 4 and 5, respectively. The plots for MT-S and MT-C blends with lower slag and cement contents are not shown here since their calorimetric responses were found to be similar with expected variations in the magnitudes of peak heat release rates and their temporal occurrence. Table 3 provides a comprehensive summary of the salient observations obtained from the isothermal calorimetry tests for all the blends used in this study. An increase in slag or cement content is found to increase the peak heat release rate and cumulative heat released, attributable to an increase in the amount of Ca2+ ions that combine with [SiO4]4- ions liberated from sodium silicate, enhancing the amount of early hydration product formation (Jiang et al., 2022; Shi and Day, 1995). The increase is more prominent in MT-C blends. For instance, the peak heat released increased from 6.8 mW/g for 10% cement blend to 16.5 mW/g for a 30% cement blend (see Table 3), both prepared with activator solutions having n of 0.10 and M_s of 1.5. Additionally, it is noticed that the cement-containing blends show significantly higher initial heat release peak in comparison to their slag counterparts, because of cement's higher reactivity. These results are also in accordance with the observations on setting times, where the MT-C blends were found to set faster than the corresponding MT-S blends. Even though the calorimetric response cannot be directly related to the setting times with high confidence (Ravikumar and Neithalath, 2012), the differences in reactivities of cement and slag provide ample evidence to substantiate this observation.

In general, the calorimetric response for MT-S blends with an M_s value of 1.0 show a single major heat release peak at all replacement levels, attributable to the combination of both wetting and dissolution of slag particles, and the formation of early reaction products, as reported earlier (Ravikumar and Neithalath, 2012). Only two exceptions from this behavior are noted: binders with slag replacement levels of 20% and 30%, at an n value of 0.05 (shown in Figure 4(a) for the 30% slag binder). Here, the first narrow peak within the first few hours of mixing corresponds to the wetting and dissolution of the

Ca-bearing compounds (Ravikumar and Neithalath, 2012; Shi and Day, 1995). The initial peak is followed by a dormant period which is succeeded by an acceleration peak that is smaller in magnitude and is generally attributed to the formation of reaction products such as calcium silicate hydrate (C-S-H) and calcium aluminosilicate hydrate (C-A-S-H) gels (Chithiraputhiran and Neithalath, 2013; Zuo and Ye, 2020). Note that these secondary peaks are observed at 9 h and 13.4 h for MT-S blends with 30% and 20% slag content, respectively. Since the time of occurrence of secondary peak increased with a decrease in slag content in the mix, there is a possibility that the secondary peak for the MT-S blend with 10% slag content may have occurred at a time greater than 48 h (as reported in another study (Jiang et al., 2022)), which was beyond the range of calorimetry experiments carried out here. For the mixtures proportioned with n values of 0.075 and 0.10, the initial peak magnitude is higher than that of the blend with an n of 0.05, but the secondary acceleration peaks are not noted here. Single peak calorimetric responses such as those shown here have been reported elsewhere (Chithiraputhiran and Neithalath, 2013; Ravikumar and Neithalath, 2012), the reason being that, in addition to wetting and dissolution of slag, formation of aluminosilicate complexes that incorporate the alkali and calcium ions also happen very early on due to the high amounts of [SiO₄]⁴ ions, which is also corroborated by the faster setting of these mixtures. MT-S blends prepared with an activator M_s of 1.5 demonstrate lower initial heat release peak magnitudes compared to those prepared with an M_s of 1.0 at the same n value and replacement level. This is also attributed to the higher alkalinity of the binder system when lower activator M_s is used. While for the blends with an M_s value of 1.0, only one wetting/dissolution/product formation peak is generally identified as shown in Figure 4(a), secondary peaks are observed for more number of binder systems when a lower M_s value of 1.5 is used, especially when the overall alkalinity of the binder system is low (i.e., n values ranging from 0.025 to 0.075). The duration between wetting/dissolution and early product formation peaks was observed to be around 35 min for all the MT-S blends prepared with an M_s of 1.5. This is likely a result of the presence of more soluble silicates in systems with higher M_s (Shi and Day, 1995). At higher alkalinities, two-peak response is not noted, since the heat release due to wetting and dissolution, and formation of reaction products overlaps. It is also possible that at higher alkalinity levels (achieved by increasing n values at a fixed replacement level and M_s value), the larger early peak masks the subsequent peak (in some cases detected as a shoulder in the main peak), an observation reported elsewhere as well (Jiang et al., 2022). Figures 5(a) and (b) depict the cumulative heat released for the MT-S blends. The heat release for the lowest n value is negligible, but at n values greater than or equal to 0.05, there is a significant increase in cumulative heat released until 48 h. The difference is rather insignificant with n values when the activator M_s is higher.

The calorimetric response curves for MT-C blends, shown in Figures 4(c) and (d) are also similar to those of the MT-S blends. Secondary peaks are observed for the blends prepared with lower n values (0.025 to 0.05), which are likely the acceleration peaks corresponding to the hydration of cement. For all replacement levels and both the M_s values, the secondary peaks are observed for blends with an n value of 0.025 within first 4 h of the test, attributable to the lower alkalinity levels. For all MT-C blends, there is an increase in peak heat release rate and cumulative heat released when the alkalinity is increased (i.e., with increase in n values at the same M_s and cement content) since more Ca^{2+} ions are introduced into the system aiding in the formation of more C-S-H and C-A-S-H gels. In general, the heat release curves of the MT-C blends can be considered to be similar to dilute cement systems, but with the acceleration effect appearing very early on, because of the influence of alkaline activators. As expected, the cumulative heat released is higher for the MT-C systems as compared to the MT-S systems as shown in Figures 5(c) and (d), because of the exothermic cement reactions.

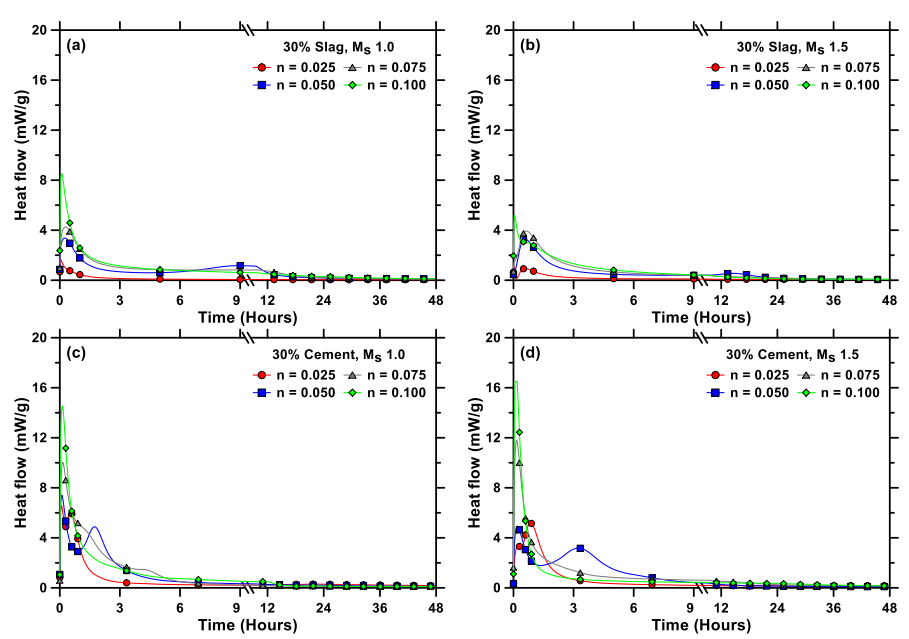


Figure 4: Heat release rate curves for: 30% slag blends prepared with an M_s value of (a) 1.0 and, (b) 1.5; 30% cement blends prepared with an M_s value of (c) 1.0 and, (d) 1.5.

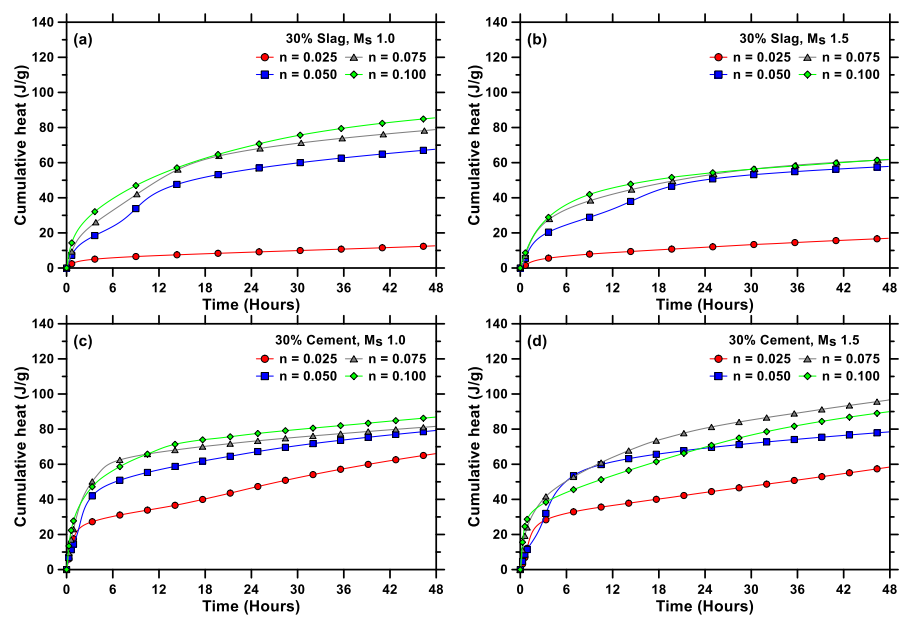


Figure 5: Cumulative heat flow curves for: 30% slag blends prepared with an M_s value of (a) 1.0 and, (b) 1.5; 30% cement blends prepared with an M_s value of (c) 1.0 and, (d) 1.5.

Table 3: Heat release response parameters of MT-S and MT-C blend pastes.

D: 1	Activation		Magnitu	de of peak	TD: .	Cumulative	
Binder	paran	neters	(mW/g)		Time to	o peak (h)	heat (J/g
composition	M_s	n	First peak	Second peak	First peak	Second peak	binder)
i		0.025	2.02	-	0.03	-	10.38
	1.0	0.050	2.72	-	0.05	-	39.40
00.14	1.0	0.075	4.18	-	0.05	-	43.19
90 Mine	-	0.100	6.90	-	0.07	-	46.17
tailing (MT) - 10 slag (S)		0.025	1.91	0.90	0.02	0.63	12.76
10 stag (3)	1.5	0.050	2.09	1.59	0.02	0.62	38.79
	1.5	0.075	5.17	-	0.02	-	43.36
		0.100	4.42	-	0.03	-	46.00
		0.025	3.16	-	0.05	-	13.76
	1.0	0.050	4.88	0.63	0.12	13.40	53.41
00.14:	1.0	0.075	5.90	-	0.12	-	65.89
80 Mine		0.100	6.82	-	0.10	-	64.47
tailing (MT) - 20 slag (S)		0.025	3.01	-	0.02	-	17.00
20 stag (3)	1.5	0.050	0.81	2.49	0.02	0.70	48.32
	1.5	0.075	3.30	2.89	0.02	0.60	58.97
		0.100	5.66	-	0.05	-	62.14
		0.025	1.63	-	0.05	-	12.62
	1.0	0.050	3.37	1.17	0.25	9.00	67.61
70.36		0.075	4.26	-	0.28	-	78.81
70 Mine		0.100	8.53	-	0.10	-	85.51
tailing (MT) -	1.5	0.025	1.02	0.94	0.02	0.58	16.91
30 slag (S)		0.050	0.91	3.28	0.02	0.58	57.84
		0.075	3.94	-	0.65	-	61.65
		0.100	5.19	-	0.05	-	61.85
		0.025	3.31	1.63	0.09	3.22	39.04
	1.0	0.050	5.81	-	0.13	-	41.96
0035	1.0	0.075	7.61	-	0.13	-	37.73
90 Mine		0.100	11.71	-	0.06	-	52.53
tailing (MT) - 10 cement (C)	1.5	0.025	2.31	0.72	0.20	13.12	40.65
10 cement (C)		0.050	5.82	-	0.17	-	31.73
		0.075	9.28	-	0.15	-	36.97
		0.100	6.79	-	0.21	-	46.86
		0.025	7.24	4.54	0.08	0.86	62.88
	1.0	0.050	8.81	2.22	0.08	3.43	63.61
00.75	1.0	0.075	13.91	-	0.10	-	70.85
80 Mine		0.100	13.63	-	0.11	-	68.26
tailing (MT) - 20 cement (C)		0.025	3.28	3.90	0.22	1.42	62.31
20 cement (C)	1.5	0.050	9.04	-	0.12	-	72.72
	1.5	0.075	11.24	-	0.17	-	59.83
		0.100	12.96	-	0.18	-	63.79
		0.025	6.56	6.03	0.08	0.53	66.08
	1.0	0.050	7.42	4.88	0.10	1.73	79.26
50.35	1.0	0.075	10.04	-	0.14	-	81.59
70 Mine		0.100	14.55	-	0.13	-	86.89
tailing (MT) -		0.025	3.40	5.17	0.22	0.85	58.42
30 cement (C)		0.050	4.93	3.17	0.19	3.23	78.48
	1.5	0.075	11.79	-	0.16	-	96.79
		0.100	16.50	-	0.08	-	89.98

3.4. Compressive strength

Compressive strength tests were performed on the selected set of MT-S and MT-C blends (for some blends, mixtures with n value ≥ 0.05 were only considered based on setting time criterion as discussed earlier), and are shown in Figures 6 and 7. For both MT-S and MT-C blends, the strength gain response is a function of the activator parameters and the cement or slag content in the system, as expected. The strength gain from 3 to 28 days is not very significant at lower alkalinity levels (n values of 0.025 and 0.05), whereas at higher n values of 0.075 and 0.10, there is a significant strength enhancement at 14 and 28 days as noticed from these figures.

It is seen from Figure 6 that an increase in the slag content increases the compressive strengths of MT-S blends significantly. This is because of the increased formation of C-S-H and/or C-A-S-H gels. The maximum compressive strength for MT-S blends with 10% slag content is \sim 12 MPa and attained for M_s and n values of 1.0 and 0.10, respectively, whereas the maximum compressive strengths of 24 MPa and 40 MPa are achieved for MT-S blends with 20% and 30% slag content respectively, with the same activator parameters. This suggests that a higher alkalinity (i.e., a lower M_s value and a higher n value) in the mixture, combined with a higher slag content, is beneficial towards the attainment of higher strength values. The activation of slag is dependent on the efficiency of the alkalis in solubilizing the silica from slag – in other words, the pH-dependent solubility of Si is an important thermodynamic factor influencing slag activation (Song and Jennings, 1999). For MT-C blends, a similar trend of increasing strength with increasing cement content is not observed, which can be attributed to the varying l/b ratios used for each replacement level (necessitated by the need to mitigate rapid setting, and allow desired workability). The highest compressive strength among the MT-C blends that were castable, was \sim 11 MPa, for a mixture with 20% cement content.

For both MT-S and MT-C blends, the compressive strength is generally found to increase with an increase in n value. This is because the water-impermeable layer on the surface of binder particles is disturbed by the alkaline activator, leading to faster reaction rates and formation of more reaction products (Bakharev, 2005; Obenaus-Emler et al., 2020). Moreover, at a higher n value, more sodium silicate is present in the activator solution, resulting in the formation of more silica-containing gel (due to higher concentration of [SiO₄]⁴ ions), lowering the Ca/Si ratio of the reaction products, which is also reported to result in higher compressive strengths (Vance et al., 2014). A similar reasoning can be used to explain the higher strengths of MT-S binders proportioned using an activator with an M_s of 1.0, as opposed to one with an M_s of 1.5. However, in certain cases, higher NaOH concentration, represented by an n value of 0.10, is seen to result in a reduction in compressive strength (seen in Figures 6 (d, f) and 6 (a, d)). This may be attributed either to the suppression of Ca²⁺ ion dissolution (Huseien et al., 2018; Phoo-ngernkham et al., 2015) and/or to the accelerated dissolution of silica and alumina which hinders the polycondensation process to form hydration products (Zuhua et al., 2009). Furthermore, the solubility reduction of Ca under higher alkalinity leads to the precipitation of calcium hydroxide (CH). Since the Ca ions are not available for the formation of C-S-H gel and instead precipitate as CH, strength gain is inhibited for the very high n value binders. This is especially noticed in some of the MT-C

Based on the foregoing discussions, for MT-S blends, it is possible to produce sustainable binders containing a high volume of MT with 28-day strengths ranging from 10-40 MPa for myriad applications through appropriate mixture design. For MT-C blends the 28-day compressive strength values are rather low, attributable to the higher l/b ratios (0.40, 0.45, and 0.55) that are used to obtain sufficient workability and flowability. Here, a higher M_s value is seen to produce slightly higher strengths, especially at higher cement contents. The strength of 40 MPa obtained this work is sufficient for a variety of structural applications including shield tunnel grouting, high strength grouting of machinery, structural steel and precast concrete, wind turbines, repair mortars and grouts etc. Hence the use of MT-S blends is a potential method to beneficially use a large volume of mine tailings in cementing materials,

towards ensuring sustainable concretes. The use of these blends for precast concrete applications including masonry blocks and tiles, and panels for residential and commercial building and infrastructure applications is also possible. Table 4 summarizes the different applications of MT-based binders for high-volume use in grouting and precast structural applications. While the strength ranges achieved here enable these mixtures to be used in cast-in-place structural concrete applications, they are deliberately not included here due to the fact that mixing and handling large volumes of alkaliactivated mixtures would need special equipment and precautions. For precast applications in factories, and small volumes such as grouts, such precautions can be easily implemented. Our ongoing work evaluates the leaching behavior, shrinkage characteristics, and durability properties, along with lifecycle cost and impact analyses of these blends to ensure their consistent and lasting performance when used in appropriate situations.

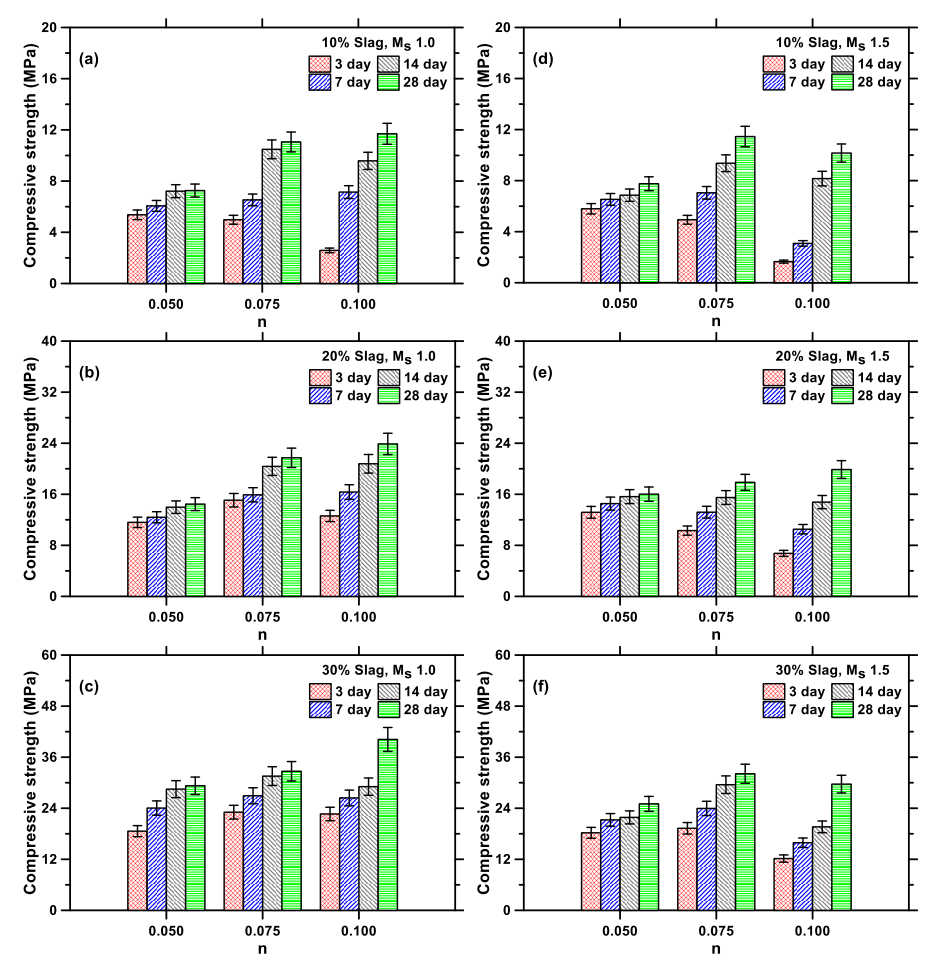


Figure 6: Compressive strengths: M_s value of 1.0 and slag contents of: (a) 10%, (b) 20%, (c) 30%; M_s value of 1.5 and slag contents of (d) 10%, (e) 20%, (f) 30%.

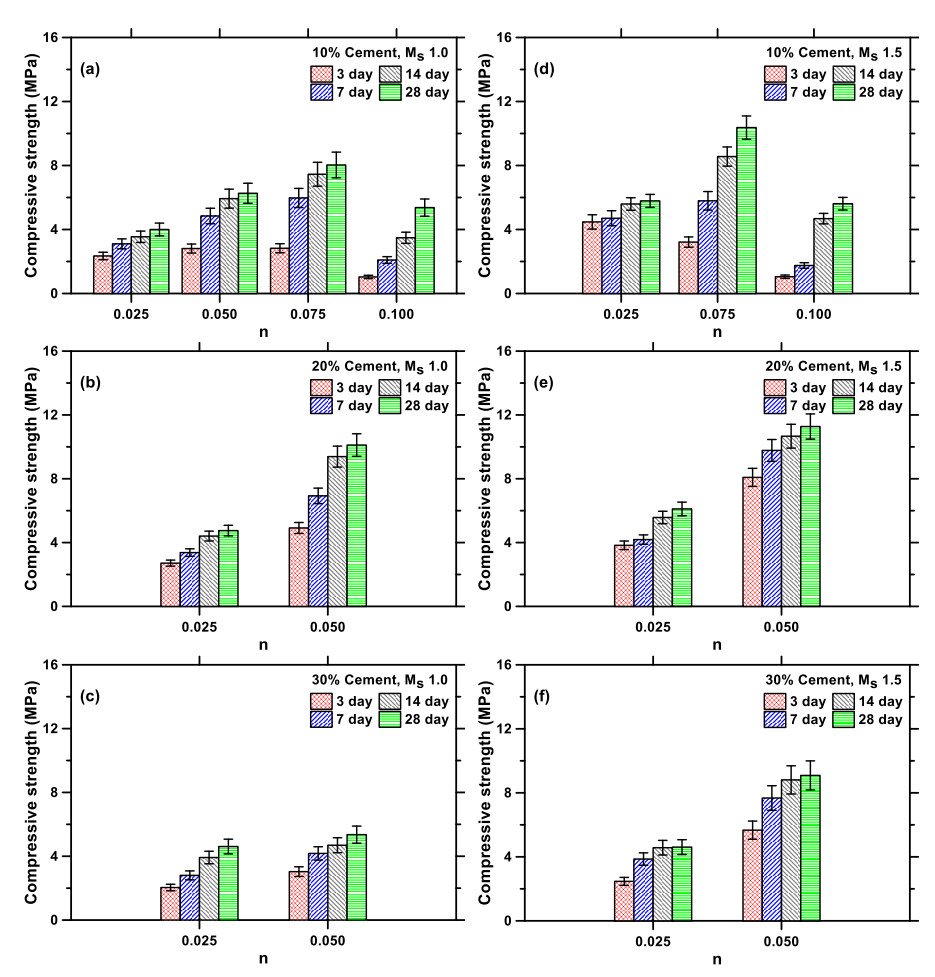


Figure 7: Compressive strengths: M_s value of 1.0 and cement contents of: (a) 10%, (b) 20%, (c) 30%; M_s value of 1.5 and cement contents of (d) 10%, (e) 20%, (f) 30%.

Table 4: Proposed applications of the MT-S and MT-C blends based on compressive strengths: The following symbols are used: x − non-castable (< 3MPa; not selected for any use case), ● − non-structural applications such as precast, non-load-bearing/insulating panels (3-7 MPa), □ − structural masonry applications (7-14 MPa), + − grout for masonry (14-25 MPa), and ✓ − high strength grout and precast load-bearing applications (> 25 MPa). While strength is the only criterion that is considered here, this table can be augmented with information on flowability and early age reactivity as needed. The use of multiple criteria for mixture selection would further narrow down the matrix of mixtures for each potential application category.

Binder system	Activation parameters (n, M _s)	Mass percentage of slag / cement in respective blends								
		10	1%	20)%	30%				
			M_s							
		1.0	1.5	1.0	1.5	1.0	1.5			

	n						
MC	0.025	X	X	X	Х	X	X
Mine tailings	0.050			+	+	✓	✓
(MT) -slag	0.075			+	+	✓	✓
(S) blends	0.100			+	+	✓	✓
Mine tailings (MT) - cement (C)	0.025	•	•	•	•	•	•
	0.050	•	X			•	
	0.075			X	X	X	x
blends	0.100	•	•	Х	X	X	x

4. Conclusions

This study focused on developing mine tailings (MT)-based binding materials for a variety of applications, emphasizing the use of high volumes of MT, so as to advance the beneficial utilization of a material that is generally landfilled in large quantities. In order to eliminate difficult processing options such as heat curing to attain desirable properties, this study explored binders that employed small amounts of a reactive (calcium) aluminosilicate such as slag (S) or cement (C) in conjunction with a large volume of MT. The dependence of the selected fresh and hardened properties of the alkali activated MT-S and MT-C blends on the alkali activation parameters (M_s and n values) and slag or cement content were studied in detail. Setting times and flowability of the binders that are critical in their potential use as grouting materials, and the early-age reactivity and their time-dependent strength development under normal curing conditions, that dictate their applicability in a range of precast construction applications (to circumvent field issues associated with the use of caustic alkalis as well as elevated temperature curing), were evaluated.

In general, the MT-S blends showed higher initial and final setting times compared to MT-C blends. For the MT-S binders, the fastest set occurred for a 30% slag blend prepared using an activation solution with M_s of 1.0 and n of 0.05, respectively, while for the MT-C blends, the fastest set was achieved at a 30% cement content mixture prepared using an activation solution with M_s of 1.5 and n of 0.075. Higher flowability was observed in mixtures with an n value of 0.05 for both M_s at all slag contents used in this work. MT-S blends were flowable for a longer period of time compared to the respective MT-C blends which lost their flowability in a few minutes after mixing, providing insights into the selection of these binders based on flow requirements for different applications such as grouting and precast concretes. Isothermal calorimetry revealed that the MT-C blends were more exothermic, with slightly higher cumulative heat release as compared to the MT-S blends. Single-peak or multi-peak calorimetric responses were observed depending on the additive type (cement or slag) and/or the activation parameters (n and M_s). The compressive strength of both MT-S and MT-C blends generally increased with an increase in slag or cement contents in the binder, as well as increasing n values (for $n \le 0.075$, especially for the MT-C blends). The strength development was also found to be uniquely linked to the activation parameters for both the blends - for lower n values, there was no appreciable strength development beyond 3 or 7 days, whereas at higher n values, the strengths significantly increased (sometimes by 3-4 times) between 7 and 28 days. Attainment of strengths of ~40 MPa at ≥ 70% of MT by mass opens a wide range of avenues for the beneficial use of high volumes of MT in construction applications.

Overall, it has been shown that the properties of MT-S and MT-C blends depend significantly on the activation parameters and the binder additive type. A proper understanding of the effects of these parameters on workability, reactivity, and mechanical properties enable selection of appropriate mixture parameters for desired properties and end applications. A matrix that helps rapid selection of such

binders was created; development of similar aids for engineers and precast concrete producers will help in increasing the potential uptake of mine tailings in various construction applications.

5. Author contributions

Conceptualization, N.N. and A.K.; methodology, R.K.R.J., A.S, and S.S.; validation, T.H. and S.S; formal analysis, R.K.R.J. and S.S.; investigation, R.K.R.J., A.S, and S.S.; resources, N.N.; data curation, S.S.; writing—original draft preparation, R.K.R.J and S.S.; writing—review and editing, A.K. and N.N; supervision, N.N.; project administration, N.N.; funding acquisition, N.N. All authors have read and agreed to the published version of the manuscript.

6. Acknowledgments

The authors sincerely acknowledge Freeport McMoRan Inc. for supplying the mine tailings and for financial support of this work through the NSF Engineering Research Center on Bio-Mediated and Bio-Inspired Geotechnics (CBBG) at ASU. The cement and slag used in this work were supplied by Salt River Materials Group (Phoenix Cement) and Cemex, respectively, and PQ Corp supplied the sodium silicate. Their contributions are also acknowledged.

7 References

Ahmari, S., Zhang, L., 2012. Production of eco-friendly bricks from copper mine tailings through geopolymerization. Construction and Building Materials 29, 323–331. https://doi.org/10.1016/j.conbuildmat.2011.10.048

Ahmari, S., Zhang, L., Zhang, J., 2012. Effects of activator type/concentration and curing temperature on alkali-activated binder based on copper mine tailings. J Mater Sci 47, 5933–5945. https://doi.org/10.1007/s10853-012-6497-9

Akinyemi, B.A., Alaba, P.A., Rashedi, A., 2022. Selected performance of alkali-activated mine tailings as cementitious composites: A review. Journal of Building Engineering 50, 104154. https://doi.org/10.1016/j.jobe.2022.104154

Alonso, M.M., Pasko, A., Gascó, C., Suarez, J.A., Kovalchuk, O., Krivenko, P., Puertas, F., 2018. Radioactivity and Pb and Ni immobilization in SCM-bearing alkali-activated matrices. Construction and Building Materials 159, 745–754. https://doi.org/10.1016/j.conbuildmat.2017.11.119

Araujo, F.S.M., Taborda-Llano, I., Nunes, E.B., Santos, R.M., 2022. Recycling and Reuse of Mine Tailings: A Review of Advancements and Their Implications. Geosciences 12, 319. https://doi.org/10.3390/geosciences12090319

Aseniero, J.P.J., Opiso, E.M., Banda, M.H.T., Tabelin, C.B., 2018. Potential utilization of artisanal gold-mine tailings as geopolymeric source material: preliminary investigation. SN Appl. Sci. 1, 35. https://doi.org/10.1007/s42452-018-0045-4

Bakharev, T., 2005. Geopolymeric materials prepared using Class F fly ash and elevated temperature curing. Cement and Concrete Research 35, 1224–1232. https://doi.org/10.1016/j.cemconres.2004.06.031

Bakharev, T., Sanjayan, J.G., Cheng, Y.-B., 2003. Resistance of alkali-activated slag concrete to acid attack. Cement and Concrete Research 33, 1607–1611. https://doi.org/10.1016/S0008-8846(03)00125-X

Barzegar Ghazi, A., Jamshidi-Zanjani, A., Nejati, H., 2022. Utilization of copper mine tailings as a partial substitute for cement in concrete construction. Construction and Building Materials 317, 125921. https://doi.org/10.1016/j.conbuildmat.2021.125921

Bernal, S.A., Mejía de Gutiérrez, R., Provis, J.L., 2012. Engineering and durability properties of concretes based on alkali-activated granulated blast furnace slag/metakaolin blends. Construction and Building Materials 33, 99–108. https://doi.org/10.1016/j.conbuildmat.2012.01.017

Brady, J.F., 1993. The rheological behavior of concentrated colloidal dispersions. The Journal of Chemical Physics 99, 567–581.

Calderon, A.R.M., Alorro, R.D., Tadesse, B., Yoo, K., Tabelin, C.B., 2020. Repurposing of nickeliferous pyrrhotite from mine tailings as magnetic adsorbent for the recovery of gold from chloride solution. Resources, Conservation and Recycling 161, 104971. https://doi.org/10.1016/j.resconrec.2020.104971

Chithiraputhiran, S., Neithalath, N., 2013. Isothermal reaction kinetics and temperature dependence of alkali activation of slag, fly ash and their blends. Construction and Building Materials 45, 233–242. https://doi.org/10.1016/j.conbuildmat.2013.03.061

Dakhane, A., Das, S., Kailas, S., Neithalath, N., 2016. Elucidating the Crack Resistance of Alkali-Activated Slag Mortars Using Coupled Fracture Tests and Image Correlation. Journal of the American Ceramic Society 99, 273–280. https://doi.org/10.1111/jace.13960

Dakhane, A., Tweedley, S., Kailas, S., Marzke, R., Neithalath, N., 2017. Mechanical and microstructural characterization of alkali sulfate activated high volume fly ash binders. Materials & Design 122, 236–246. https://doi.org/10.1016/j.matdes.2017.03.021

Ercikdi, B., Cihangir, F., Kesimal, A., Deveci, H., 2017. Practical Importance of Tailings for Cemented Paste Backfill, in: Yilmaz, E., Fall, M. (Eds.), Paste Tailings Management. Springer International Publishing, Cham, pp. 7–32. https://doi.org/10.1007/978-3-319-39682-8 2

Fernández-Jiménez, A., Palomo, J.G., Puertas, F., 1999. Alkali-activated slag mortars: Mechanical strength behaviour. Cement and Concrete Research 29, 1313–1321. https://doi.org/10.1016/S0008-8846(99)00154-4

Guo, J., Bao, Y., Wang, M., 2018. Steel slag in China: Treatment, recycling, and management. Waste Management 78, 318–330. https://doi.org/10.1016/j.wasman.2018.04.045

Hageman, P.L., Briggs, P.H., 2000. A simple field leach test for rapid screening and qualitative characterization of mine waste dump material on abandoned mine lands (No. 2000–15), Open-File Report. U.S. Dept. of the Interior, U.S. Geological Survey, https://doi.org/10.3133/ofr0015

Huseien, G.F., Ismail, M., Khalid, N.H.A., Hussin, M.W., Mirza, J., 2018. Compressive strength and microstructure of assorted wastes incorporated geopolymer mortars: Effect of solution molarity. Alexandria Engineering Journal 57, 3375–3386. https://doi.org/10.1016/j.aej.2018.07.011

Jamshidi-Zanjani, A., Saeedi, M., 2013. Metal pollution assessment and multivariate analysis in sediment of Anzali international wetland. Environ Earth Sci 70, 1791–1808. https://doi.org/10.1007/s12665-013-2267-5

Jiang, D., Shi, C., Zhang, Z., 2022. Recent progress in understanding setting and hardening of alkaliactivated slag (AAS) materials. Cement and Concrete Composites 134, 104795. https://doi.org/10.1016/j.cemconcomp.2022.104795

Jiang, L., Sun, H., Peng, T., Ding, W., Liu, B., Liu, Q., 2021. Comprehensive evaluation of environmental availability, pollution level and leaching heavy metals behavior in non-ferrous metal tailings. Journal of Environmental Management 290, 112639. https://doi.org/10.1016/j.jenvman.2021.112639

- Jiang, X., Liu, W., Xu, H., Cui, X., Li, J., Chen, J., Zheng, B., 2021. Characterizations of heavy metal contamination, microbial community, and resistance genes in a tailing of the largest copper mine in China. Environmental Pollution 280, 116947. https://doi.org/10.1016/j.envpol.2021.116947
- Kiventerä, J., Perumal, P., Yliniemi, J., Illikainen, M., 2020. Mine tailings as a raw material in alkali activation: A review. International Journal of Minerals, Metallurgy and Materials 27, 1009–1020. https://doi.org/10.1007/s12613-020-2129-6
- Koohestani, B., Mokhtari, P., Yilmaz, E., Mahdipour, F., Darban, A.K., 2021. Geopolymerization mechanism of binder-free mine tailings by sodium silicate. Construction and Building Materials 268, 121217. https://doi.org/10.1016/j.conbuildmat.2020.121217
- Kovalchuk, G., Fernández-Jiménez, A., Palomo, A., 2007. Alkali-activated fly ash: Effect of thermal curing conditions on mechanical and microstructural development Part II. Fuel 86, 315–322. https://doi.org/10.1016/j.fuel.2006.07.010
- Krishna, R.S., Shaikh, F., Mishra, J., Lazorenko, G., Kasprzhitskii, A., 2021. Mine tailings-based geopolymers: Properties, applications and industrial prospects. Ceramics International 47, 17826–17843. https://doi.org/10.1016/j.ceramint.2021.03.180
- Krishna, R. S., Shaikh, F., Mishra, J., Lazorenko, G., Kasprzhitskii, A., 2021. Mine tailings-based geopolymers: Properties, applications and industrial prospects. Ceramics International 47, 17826–17843. https://doi.org/10.1016/j.ceramint.2021.03.180
- Lakrat, M., Mejdoubi, E.M., Ozdemir, F., Santos, C., 2022. Effect of sodium silicate concentration on the physico-chemical properties of dual-setting bone-like apatite cements. Materials Today Communications 31, 103421. https://doi.org/10.1016/j.mtcomm.2022.103421
- Lèbre, É., Corder, G.D., Golev, A., 2017. Sustainable practices in the management of mining waste: A focus on the mineral resource. Minerals Engineering, Sustainable Minerals 107, 34–42. https://doi.org/10.1016/j.mineng.2016.12.004
- Lee, S.K., Stebbins, J.F., 2003. The distribution of sodium ions in aluminosilicate glasses: a high-field Na-23 MAS and 3Q MAS NMR study. Geochimica et Cosmochimica Acta 67, 1699–1709. https://doi.org/10.1016/S0016-7037(03)00026-7
- Liu, Q., Cui, M., Li, X., Wang, J., Wang, Z., Li, L., Lyu, X., 2022. Alkali-hydrothermal activation of mine tailings to prepare one-part geopolymer: Activation mechanism, workability, strength, and hydration reaction. Ceramics International 48, 30407–30417. https://doi.org/10.1016/j.ceramint.2022.06.318
- Marove, C.A., Sotozono, R., Tangviroon, P., Tabelin, C.B., Igarashi, T., 2022. Assessment of soil, sediment and water contaminations around open-pit coal mines in Moatize, Tete province, Mozambique. Environmental Advances 8, 100215. https://doi.org/10.1016/j.envadv.2022.100215
- Niu, H., Helser, J., Corfe, I.J., Kuva, J., Butcher, A.R., Cappuyns, V., Kinnunen, P., Illikainen, M., 2022. Incorporation of bioleached sulfidic mine tailings in one-part alkali-activated blast furnace slag mortar. Construction and Building Materials 333, 127195. https://doi.org/10.1016/j.conbuildmat.2022.127195
- Obenaus-Emler, R., Falah, M., Illikainen, M., 2020. Assessment of mine tailings as precursors for alkali-activated materials for on-site applications. Construction and Building Materials 246, 118470. https://doi.org/10.1016/j.conbuildmat.2020.118470
- Opiso, E.M., Tabelin, C.B., Maestre, C.V., Aseniero, J.P.J., Park, I., Villacorte-Tabelin, M., 2021. Synthesis and characterization of coal fly ash and palm oil fuel ash modified artisanal and small-scale

gold mine (ASGM) tailings based geopolymer using sugar mill lime sludge as Ca-based activator. Heliyon 7. https://doi.org/10.1016/j.heliyon.2021.e06654

Opiso, E.M., Tabelin, C.B., Ramos, L.M., Gabiana, L.J.R., Banda, M.H.T., Delfinado, J.R.Y., Orbecido, A.H., Zoleta, J.B., Park, I., Arima, T., Villacorte-Tabelin, M., 2023. Development of a three-step approach to repurpose nickel-laterite mining waste into magnetite adsorbents for As(III) and As(V) removal: Synthesis, characterization and adsorption studies. Journal of Environmental Chemical Engineering 11, 108992. https://doi.org/10.1016/j.jece.2022.108992

Ouffa, N., Trauchessec, R., Benzaazoua, M., Lecomte, A., Belem, T., 2022. A methodological approach applied to elaborate alkali-activated binders for mine paste backfills. Cement and Concrete Composites 127, 104381. https://doi.org/10.1016/j.cemconcomp.2021.104381

Pacheco-Torgal, F., Abdollahnejad, Z., Camões, A.F., Jamshidi, M., Ding, Y., 2012. Durability of alkali-activated binders: A clear advantage over Portland cement or an unproven issue? Construction and Building Materials 30, 400–405. https://doi.org/10.1016/j.conbuildmat.2011.12.017

Park, I., Tabelin, C.B., Jeon, S., Li, X., Seno, K., Ito, M., Hiroyoshi, N., 2019. A review of recent strategies for acid mine drainage prevention and mine tailings recycling. Chemosphere 219, 588–606. https://doi.org/10.1016/j.chemosphere.2018.11.053

Perumal, P., Niu, H., Kiventerä, J., Kinnunen, P., Illikainen, M., 2020. Upcycling of mechanically treated silicate mine tailings as alkali activated binders. Minerals Engineering 158, 106587. https://doi.org/10.1016/j.mineng.2020.106587

Phoo-ngernkham, T., Sata, V., Hanjitsuwan, S., Ridtirud, C., Hatanaka, S., Chindaprasirt, P., 2015. High calcium fly ash geopolymer mortar containing Portland cement for use as repair material. Construction and Building Materials 98, 482–488. https://doi.org/10.1016/j.conbuildmat.2015.08.139

Provis, J.L., 2018. Alkali-activated materials. Cement and Concrete Research 114, 40–48. https://doi.org/10.1016/j.cemconres.2017.02.009

Qaidi, S.M.A., Tayeh, B.A., Zeyad, A.M., de Azevedo, A.R.G., Ahmed, H.U., Emad, W., 2022. Recycling of mine tailings for the geopolymers production: A systematic review. Case Studies in Construction Materials 16, e00933. https://doi.org/10.1016/j.cscm.2022.e00933

Rao, F., Liu, Q., 2015. Geopolymerization and Its Potential Application in Mine Tailings Consolidation: A Review. Mineral Processing and Extractive Metallurgy Review 36, 399–409. https://doi.org/10.1080/08827508.2015.1055625

Ravikumar, D., Neithalath, N., 2012. Reaction kinetics in sodium silicate powder and liquid activated slag binders evaluated using isothermal calorimetry. Thermochimica Acta 546, 32–43. https://doi.org/10.1016/j.tca.2012.07.010

Ravikumar, D., Peethamparan, S., Neithalath, N., 2010. Structure and strength of NaOH activated concretes containing fly ash or GGBFS as the sole binder. Cement and Concrete Composites 32, 399–410. https://doi.org/10.1016/j.cemconcomp.2010.03.007

Ruiz-Sánchez, A., Tapia, J.C.J., Lapidus, G.T., 2023. Evaluation of acid mine drainage (AMD) from tailings and their valorization by copper recovery. Minerals Engineering 191, 107979. https://doi.org/10.1016/j.mineng.2022.107979

Rzymski, P., Klimaszyk, P., Marszelewski, W., Borowiak, D., Mleczek, M., Nowiński, K., Pius, B., Niedzielski, P., Poniedziałek, B., 2017. The chemistry and toxicity of discharge waters from copper mine tailing impoundment in the valley of the Apuseni Mountains in Romania. Environ Sci Pollut Res Int 24, 21445–21458. https://doi.org/10.1007/s11356-017-9782-y

- Saedi, A., Jamshidi-Zanjani, A., Darban, A.K., Mohseni, M., Nejati, H., 2022. Utilization of lead–zinc mine tailings as cement substitutes in concrete construction: Effect of sulfide content. Journal of Building Engineering 57, 104865. https://doi.org/10.1016/j.jobe.2022.104865
- Shi, C., Day, R.L., 1995. A calorimetric study of early hydration of alkali-slag cements. Cement and Concrete Research 25, 1333–1346. https://doi.org/10.1016/0008-8846(95)00126-W
- Song, S., Jennings, H.M., 1999. Pore solution chemistry of alkali-activated ground granulated blast-furnace slag11This paper was originally submitted to Advanced Cement Based Materials. The paper was received at the Editorial Office of Cement and Concrete Research on 12 November 1998 and accepted in final form on 16 November 1998. Cement and Concrete Research 29, 159–170. https://doi.org/10.1016/S0008-8846(98)00212-9
- Surehali, S., Han, T., Huang, J., Kumar, A., Neithalath, N., 2024. On the use of machine learning and data-transformation methods to predict hydration kinetics and strength of alkali-activated mine tailings-based binders. Construction and Building Materials 419, 135523. https://doi.org/10.1016/j.conbuildmat.2024.135523
- Surehali, S., Simon, A., Ramasamy, R.K., Neithalath, N., 2023. A Comparison of the Effect of Activator Cations (Sodium and Potassium) on the Fresh and Hardened Properties of Mine Tailing-Slag Binders. Construction Materials 3, 389–404. https://doi.org/10.3390/constrmater3040025
- Tabelin, C.B., Dallas, J., Casanova, S., Pelech, T., Bournival, G., Saydam, S., Canbulat, I., 2021a. Towards a low-carbon society: A review of lithium resource availability, challenges and innovations in mining, extraction and recycling, and future perspectives. Minerals Engineering 163, 106743. https://doi.org/10.1016/j.mineng.2020.106743
- Tabelin, C.B., Park, I., Phengsaart, T., Jeon, S., Villacorte-Tabelin, M., Alonzo, D., Yoo, K., Ito, M., Hiroyoshi, N., 2021b. Copper and critical metals production from porphyry ores and E-wastes: A review of resource availability, processing/recycling challenges, socio-environmental aspects, and sustainability issues. Resources, Conservation and Recycling 170, 105610. https://doi.org/10.1016/j.resconrec.2021.105610
- Tabelin, C.B., Silwamba, M., Paglinawan, F.C., Mondejar, A.J.S., Duc, H.G., Resabal, V.J., Opiso, E.M., Igarashi, T., Tomiyama, S., Ito, M., Hiroyoshi, N., Villacorte-Tabelin, M., 2020. Solid-phase partitioning and release-retention mechanisms of copper, lead, zinc and arsenic in soils impacted by artisanal and small-scale gold mining (ASGM) activities. Chemosphere 260, 127574. https://doi.org/10.1016/j.chemosphere.2020.127574
- Tabelin, C.B., Uyama, A., Tomiyama, S., Villacorte-Tabelin, M., Phengsaart, T., Silwamba, M., Jeon, S., Park, I., Arima, T., Igarashi, T., 2022. Geochemical audit of a historical tailings storage facility in Japan: Acid mine drainage formation, zinc migration and mitigation strategies. Journal of Hazardous Materials 438, 129453. https://doi.org/10.1016/j.jhazmat.2022.129453
- Tian, X., Rao, F., León-Patiño, C.A., Song, S., 2020. Co-disposal of MSWI fly ash and spent caustic through alkaline-activation: Immobilization of heavy metals and organics. Cement and Concrete Composites 114, 103824. https://doi.org/10.1016/j.cemconcomp.2020.103824
- US EPA, O., 2014. Technologically Enhanced Naturally Occurring Radioactive Materials (TENORM) [WWW Document]. URL https://www.epa.gov/radiation/technologically-enhanced-naturally-occurring-radioactive-materials-tenorm (accessed 5.23.23).
- Van Jaarsveld, J.G.S., Van Deventer, J.S.J., Lorenzen, L., 1997. The potential use of geopolymeric materials to immobilise toxic metals: Part I. Theory and applications. Minerals Engineering 10, 659–669. https://doi.org/10.1016/S0892-6875(97)00046-0

Vance, K., Aguayo, M., Dakhane, A., Ravikumar, D., Jain, J., Neithalath, N., 2014. Microstructural, Mechanical, and Durability Related Similarities in Concretes Based on OPC and Alkali-Activated Slag Binders. Int J Concr Struct Mater 8, 289–299. https://doi.org/10.1007/s40069-014-0082-3

Xiaolong, Z., Shiyu, Z., Hui, L., Yingliang, Z., 2021. Disposal of mine tailings via geopolymerization. Journal of Cleaner Production 284, 124756. https://doi.org/10.1016/j.jclepro.2020.124756

Yu, L., Zhang, Z., Huang, X., Jiao, B., Li, D., 2017. Enhancement Experiment on Cementitious Activity of Copper-Mine Tailings in a Geopolymer System. Fibers 5, 47. https://doi.org/10.3390/fib5040047

Zhang, F., Li, Y., Zhang, J., Gui, X., Zhu, X., Zhao, C., 2022. Effects of slag-based cementitious material on the mechanical behavior and heavy metal immobilization of mine tailings based cemented paste backfill. Heliyon 8, e10695. https://doi.org/10.1016/j.heliyon.2022.e10695

Zhang, W., Long, J., Zhang, X., Shen, W., Wei, Z., 2020. Pollution and Ecological Risk Evaluation of Heavy Metals in the Soil and Sediment around the HTM Tailings Pond, Northeastern China. International Journal of Environmental Research and Public Health 17, 7072. https://doi.org/10.3390/ijerph17197072

Zhu, Y., Wang, Z., Li, Z., Yu, H., 2022. Experimental research on the utilization of gold mine tailings in magnesium potassium phosphate cement. Journal of Building Engineering 45, 103313. https://doi.org/10.1016/j.jobe.2021.103313

Zuhua, Z., Xiao, Y., Huajun, Z., Yue, C., 2009. Role of water in the synthesis of calcined kaolin-based geopolymer. Applied Clay Science 43, 218–223. https://doi.org/10.1016/j.clay.2008.09.003

Zuo, Y., Ye, G., 2020. Preliminary Interpretation of the Induction Period in Hydration of Sodium Hydroxide/Silicate Activated Slag. Materials (Basel) 13, E4796. https://doi.org/10.3390/ma13214796